

We are IntechOpen, the world's leading publisher of Open Access books Built by scientists, for scientists

5,000

Open access books available

125,000

International authors and editors

140M

Downloads

Our authors are among the

154

Countries delivered to

TOP 1%

most cited scientists

12.2%

Contributors from top 500 universities



WEB OF SCIENCE™

Selection of our books indexed in the Book Citation Index
in Web of Science™ Core Collection (BKCI)

Interested in publishing with us?
Contact book.department@intechopen.com

Numbers displayed above are based on latest data collected.
For more information visit www.intechopen.com



The Role of Micro Vortex in the Environmental and Biological Processes

Benjamin Oyegbile, Brian Oyegbile and Guven Akdogan

Abstract

This work presents a short review of the theoretical developments in the application of vortex dynamics to the processing of environmental and biological systems. The mechanisms of complex fluid-particle interaction in vortex dominated and non-vortex dominated flows are briefly discussed from theoretical and practical perspectives. Micro vortex propagation, characteristics and their various applications in environmental process engineering are briefly discussed. Several existing and potential applications of vortex dynamics in turbulent flows are highlighted and as well as the knowledge gaps in the current understanding of turbulence phenomenon with respect to its applications in the processing of solid-liquid suspension and biological systems.

Keywords: hydrodynamics, turbulence, eddies, vortex, aggregation

1. Introduction

Hydrodynamic-mediated interactions often occur in many technical and natural environmental processes. In the case of turbulent flows, this leads to the formation of turbulent eddies of various scales and sizes [1, 2]. These energy-carrying eddies often interact with particles and biological materials on various temporal and spatial scales. Eddy-particle interactions often play a crucial role in these processes and it is largely the dominant driver of mass and momentum transfer. In studying the dynamics of such complex interplay of forces, a good knowledge of the vortex dynamics and its influence on the fluid and particle dynamics is highly indispensable [3, 4].

Turbulent mixing, particle dispersion, and bioreactions have been topics of intense and sustained interest in many scientific inquiries [5, 6]. The role of mixing and turbulence-driven particle dispersion in many fluid-particle processes is well-understood owing an abundant body of knowledge from many scientific interrogations. However, turbulence as a phenomenon is still poorly understood due to its complex nature. Since mixing and chemical reactions are impacted by the presence of turbulence, it is therefore extremely important to understand the different scales of turbulence in mixing applications.

As mentioned earlier, turbulence has been shown to lead to the formation of eddies on different scales [7, 8]. The spatial degree of mixing such as the macro, meso and micro mixing are governed by the different scales of turbulence [5]. Mixing especially at high Reynolds number is often characterized by irregular,

rotational, and dissipative motion containing vorticities of different energy spectra or eddy sizes [3]. It is therefore imperative to carry out qualitative and quantitative assessment of mixing efficiency in many of the practical applications involving mixing and dispersion. A number of techniques are available for quantifying mixing performance in a wide range of applications. One widely used parameter for quantifying the mixing performance is the coefficient of variation proposed by Alloca and Streiff [6]. This approach relies on the statistical analysis of the spatio-temporal homogeneity of the particle dispersion in mixing applications [9]. Several other techniques are also available for quantifying the degree of mixing in bioreactor systems. In terms of the different phenomena responsible for fluid-particle mixing, advective, turbulent, and diffusive transport depicted in **Figure 1** are the dominant ones.

In turbulent mixing, energy transfer occurs on different eddy scales or energy spectrum. These turbulent eddies consist of the large energy carrying eddies at the inertia sub-range to the smallest ones at the dissipation sub-range as shown in **Figure 2**. The important scales of energy spectrums with respect to the different mixing regimes (i.e. micro, meso, and macro mixing) are the Kolmogorov, Batchelor, and Taylor length scales (Eqs. (1)–(3)). The Kolmogorov length scale of turbulence is used as a convenient reference point for comparison of different scales of mixing. A detailed description of the different time and length scales in turbulent flows is beyond the scope of this work. Further discussion on the subject matter can be found in the following reference texts [11, 12]. Therefore, getting the desired mixing regime is highly imperative for enhanced mass and momentum transfer.

In fluid-particle mixing there exist three distinct mixing regimes in most practical mixing applications namely: micro, meso, and macro mixing. In typical mixing conditions, the dividing line between micro and macro scale is between 100 and 1000 μm , respectively [13]. Consequently, it is often necessary to tailor the mixing performance to the physical, chemical, and biological processes in the target reactor systems.

Macromixing is largely driven by the largest scale of motion in the fluid or the integral length scale. Meso mixing on the other hand involves mixing on a smaller scale than the bulk circulation, but larger than the micro mixing, while micro mixing refers to the mixing on the smallest scale of fluid motion or molecular level. The largest eddies in turbulent dispersion which represents the macro scale of turbulence, are produced by the stirrer or the agitator head and contains most of the fluid energy [11, 14]. Turbulent flow can be viewed as an eddy continuum, with their sizes ranging from the dimension of the turbulence generating device to the Kolmogorov length scale. In between the energy-containing and energy-dissipating

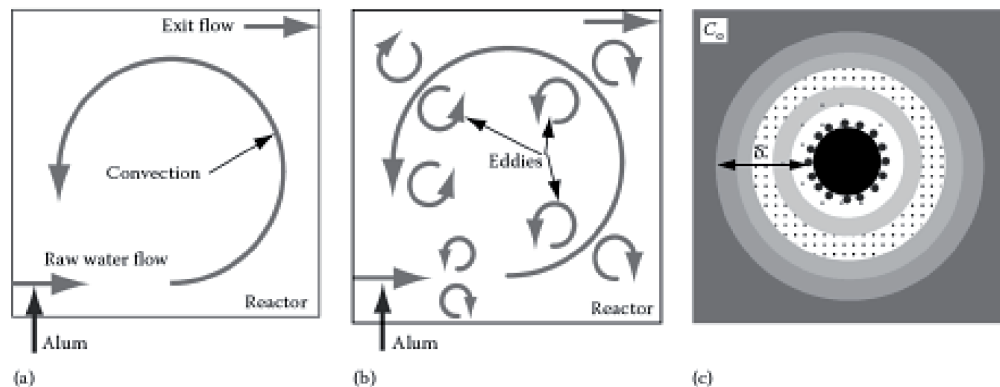


Figure 1. Schematic representation of different mixing and transport mechanisms (a) advection (b) turbulence (c) diffusion (reproduced from [10] with permissions © 2011 Taylor & Francis).

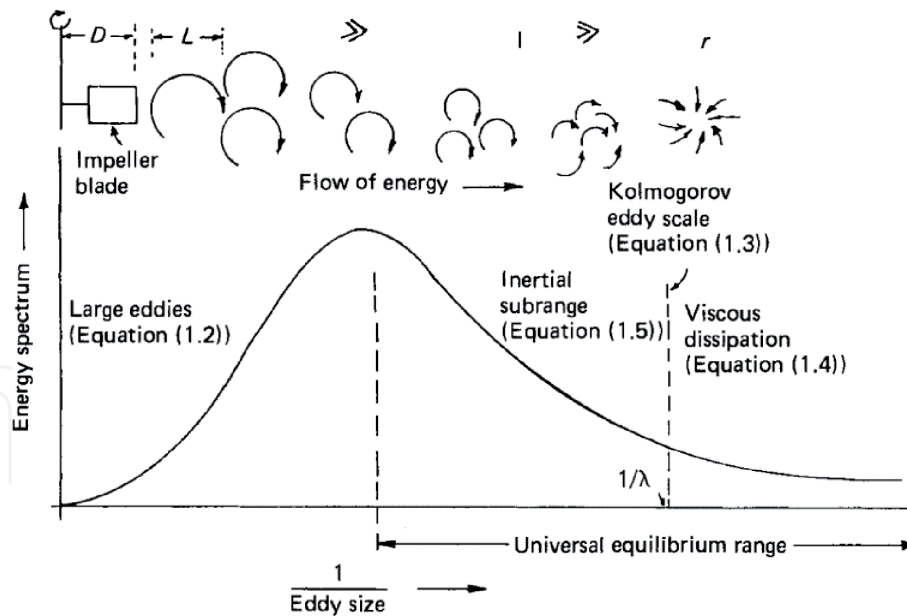


Figure 2. Schematic view of energy spectrum in turbulent mixing (reproduced from [15] with permissions © 2007 IWA publishing).

eddies, there exists many eddies of other scales smaller than the integral scale that continually transfer the kinetic energy of the fluid through the other length scales. The Batchelor and Taylor scales given in Eqs. (2) and (3) are the examples of other important length scales of fluid motion.

The Taylor scale is an intermediate length scale in the viscous subrange that is representative of the energy transfer from large to small scales, but not a dissipation scale and does not represent any distinct group of eddies. Batchelor scale on the other hand is a limiting length scale where the rate of molecular diffusion is equal to the rate of dissipation of turbulent kinetic energy of the fluid.

$$\lambda_0 = \left[\frac{v^2}{\varepsilon} \right]^{\frac{1}{4}} \quad (1)$$

$$\lambda_B = \left[\frac{D^2 v}{\varepsilon} \right]^{\frac{1}{4}} \quad (2)$$

$$\lambda_T = \frac{u\sqrt{15}}{\sqrt{\frac{\varepsilon}{v}}} \quad (3)$$

2. Colloidal stability and interaction forces

Colloidal materials in environmental and biological systems consist of small particles with very large surface area. Their typical sizes are in the range of 0.001–10 μm as shown in **Table 1**. The stability of these colloidal materials when dispersed in fluid can be explained by their tendency to acquire electrostatic charges by adsorbing ions from their surroundings. Forces mediating particle-particle interactions can broadly be classified into the following categories depending

Particle sizes, mm	Classification	Examples	Total surface area, $\text{m}^2 \text{cm}^{-3}$	Time required to settle 100 mm if $\text{SG} = 2.65$
10^{-1}	Coarse dispersion	Sand, mineral substances, precipitated and flocculated substances, silt, microplankton	6×10^{-4} – 6×10^{-2}	0.1–13 s
10^{-2} – 10^{-4}	Fine particle dispersion	Mineral substances, precipitated and flocculated substances, silt, bacteria, plankton, and other micro organisms	0.6–60	11 min–2 years
10^{-5} – 10^{-6}	Colloidal dispersion	Mineral substances, hydrolyzed and precipitated products, macromolecules, biopolymers, viruses	6×10^3	20 years
$<10^{-6}$	Solution	Inorganic simple and complex ions, molecules and polymeric species, polyelectrolytes, organic molecules and undissociated solutes	—	—

Table 1.
Classification of particles in dispersion [16].

on the chosen approach: contact forces due to the particle-particle collisions and non-contact forces due to molecular interactions at contact or interface. A brief description of these forces is hereby presented in the following sections.

2.1 Molecular dynamics approach

The molecular dynamics description of particle-particle interaction forces shown in **Figure 3** is based on the molecular interactions through interfacial forces on the surface of the interacting particles [17]. Interfacial forces are generally assumed to act on a length scales smaller than the particle size and interactions are only possible when particles are in close proximity or during collisions. The interactions of particles in suspension depend on these surface forces which consists of the long-range ionic electrostatic repulsive forces and the short-range London-van der Waals attractive forces. Classical DLVO or colloid stability theory provides a quantitative description of the forces experienced by particles in close proximity by considering such interactions forces to be additive [18].

The magnitude of the London-van der Waals attractive force between two charged particles and the electrostatic repulsive force due to the electric double layer can be derived from their corresponding interaction potential energies [17]. Eqs. (4)

and (5) represent the magnitude of these forces while Eqs. (6) and (7) represent their respective potential energies. In addition to these surface forces, a number of other interfacial interactions such as the hydration effects, hydrophobic attraction, steric repulsion, and polymer bridging have been observed to mediate particle-particle interactions [19]. Additional forces due to the fluid-particle interactions must also be considered to fully resolve all the forces experienced by particles in suspension and this is briefly discussed in Section 3.

$$F_{vdw} = \frac{dU_{vdw}}{dR_{ij}} \quad (4)$$

$$F_{elec} = \frac{dU_{elec}}{dR_{ij}} \quad (5)$$

$$U_{vdw} = \frac{A_H}{6} \left[\frac{2R_i^2}{R_{ij}^2 - 4R_i^2} + \frac{2R_i^2}{R_{ij}^2} + \ln \left\{ 1 - \frac{4R_i^2}{R_{ij}^2} \right\} \right] \quad (6)$$

$$U_{elec} = 2\pi\epsilon R_i \Psi_o^2 \ln \left[1 + \exp \left(-K(R_{ij} - 2R_i) \right) \right] \quad (7)$$

where R_{ij} is the distance between two interacting particles (center-to-center), A_H is the Hamaker constant, ϵ is the permittivity of the medium, ψ_0 is the surface potential of the particles, K is the reciprocal of the Debye length.

2.2 Micromechanical approach

In contrast to the molecular dynamics approach, the micromechanical description of particle-particle interaction relies on the geometric analysis of finite number

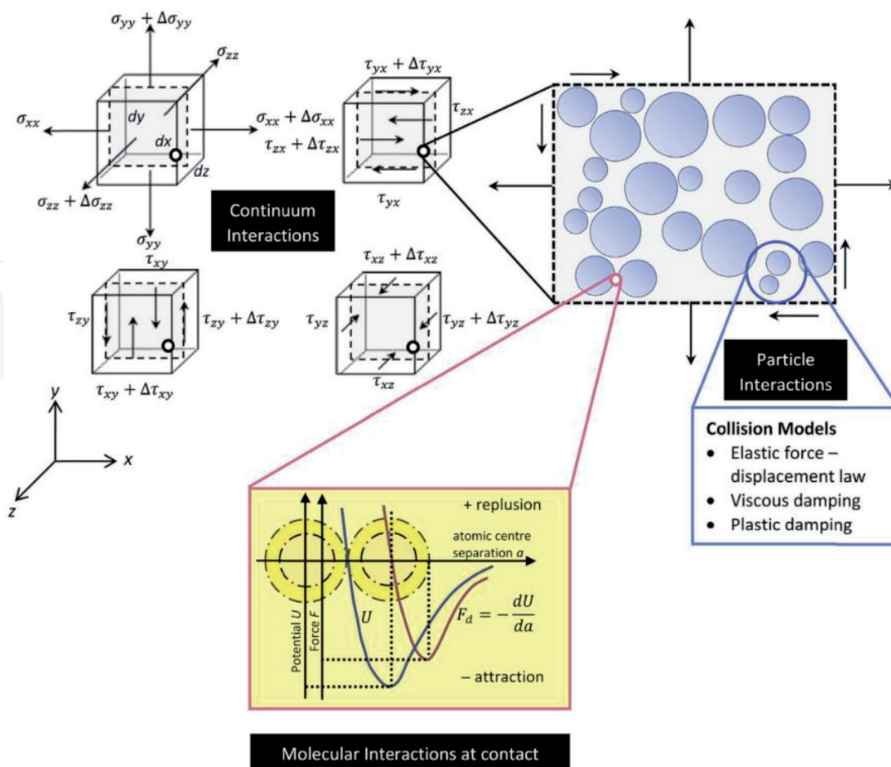


Figure 3. Classification of different phenomena fluid-particle interactions (reproduced from with [17] permissions © 2019 Elsevier).

of discrete sub-elements as shown in **Figure 3**. All particle-particle interactions within this context are described by contact forces in the normal and tangential directions, while considering the elastic force-displacement, inelastic deformations or plastic dislocations, solid friction, and viscous damping [17]. Depending on the simplicity of these interactions, a soft or hard sphere description can be given. In the hard sphere model, only elastic force-displacement is allowed. Soft sphere model on the other hand allows for most of the interactions that are possible when two particles are in direct contact.

When all these contact forces are fully resolved, the behavior of the particles upon collisions or impact on a wall such as their translational and rotational velocities can be predicted with a high degree of accuracy. A detailed description of the micromechanical theory of particle collisions and its importance in the determination of particle trajectory in dispersed suspension is beyond the scope of this communication and is available elsewhere [20]. In addition to the contact forces, body forces such as gravity and buoyancy and surface forces due to the fluid are some of the other important forces acting on the particles and their quantification is highly indispensable in resolving the dynamics of particles in suspension [21]. Some of these additional forces are discussed in the next section.

3. Particle-vortex interactions in turbulence

In order to initiate meaningful interactions through the interfacial forces, particles must be brought in close proximity. This can be achieved through the mechanisms of Brownian motion, differential settling, or turbulent dispersion as shown in **Figure 4**. The probability of particle collisions and the frequency of such collisions also depend on the trajectory of the particle motion. Thomas et al. [22] identified two types of particle trajectories leading to particle collisions namely: curvilinear and rectilinear particle trajectories. The particles in suspension under the influence of turbulence will experience fluctuating fluid motion with the particle being transported by the fluid eddies that exists within the flow vortex [3].

Consequently, small particles suspended in fluid exist in an environment of small energy-dissipating eddies in most practical flow devices. Under such conditions, particle collisions are facilitated by eddy size similar to that of the colliding particles. Furthermore, studies have shown that in addition to the fluid properties,

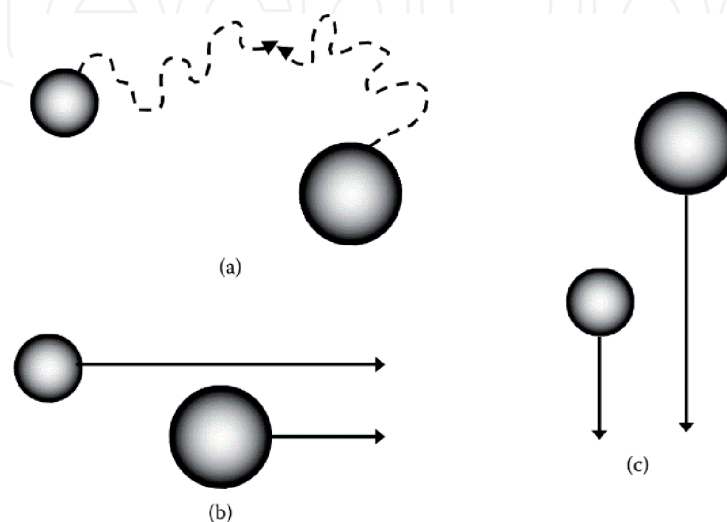


Figure 4. Mechanisms of particle transport in fluid leading to collisions (a) Brownian motion (b) fluid turbulence (c) differential settling (reproduced from [19] with permissions © 2006 CRC press).

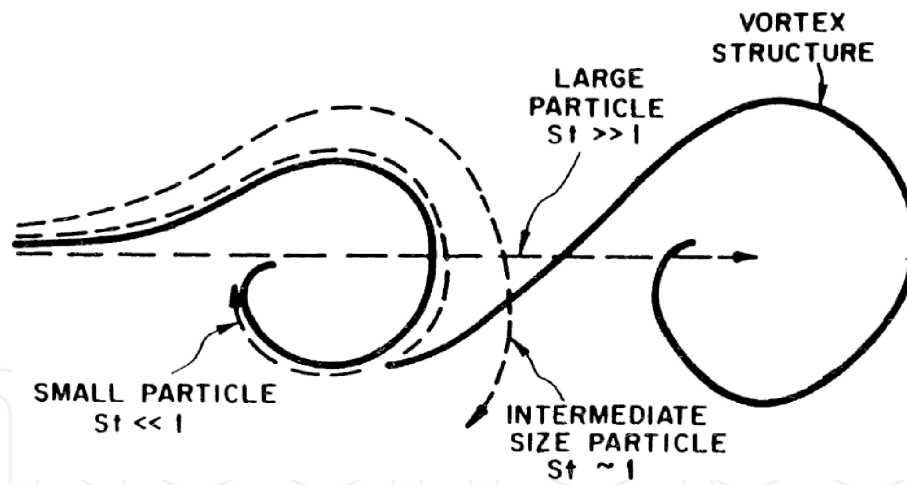


Figure 5. Vortex-Particle interactions in turbulent flow (reproduced from [1] with permissions © 1995 springer).

the particle properties such as size, density, and porosity also play important role in particle-vortex interactions [1, 23]. Smaller particles with lower density than the flow fluid have been shown to be fully entrained within the vortex in the case of a vortical flow produced by the interaction of two flow streams of unequal velocity. The particles will be in dynamic equilibrium with the carrier fluid and will faithfully follow the flow streamlines. On the other hand, large particles will be unaffected by the vortex due to their large inertia, while the intermediate particles will be driven from the center of the vortex to the periphery as shown in **Figure 5**. The determining factor in particle-vortex interactions is the ratio of the particle relaxation time to that of the fluid, which is given by the Stokes number (Eq. (8)). Depending on the flow scenario, the particles in suspension will experience additional forces such as the drag, lift, pressure gradient, virtual mass, basset, and viscous stress forces due to the fluid-particle interactions [4, 24]. Taken together, all these forces will ultimately determine the trajectory, dynamics, and fate of particles in suspension. The trajectory equation is given in Eq. (9).

$$St = \frac{\tau_A}{\tau_F} = \frac{\rho_p d^2 U}{18\mu L} \quad (8)$$

where is τ_A the particle relaxation time, τ_F is the time associated with fluid motion (fluid time), ρ_p is the particle density, d is the particle diameter, L is the length scale associated with the vortex while U is the flow velocity.

$$m \frac{d\vec{v}}{dt} = \vec{F}_{mol} + \vec{F}_{mic} + \vec{F}_{f-p} \quad (9)$$

4. Particle dynamics and aggregate disruption

Turbulence is the main driver of particle interactions in many practical applications. Consequently, the particle dynamics in terms of the particle collisions, coalescence/aggregation, growth, and breakage is primarily controlled by the fluid turbulence. The aggregate stability under the influence of hydrodynamic force has been suggested to be a function of the binding or cohesive force F_B and

the hydrodynamic breaking force F_H . While the binding force is determined by the aggregate structure and physicochemical attributes discussed Section 2, flow turbulence is the principal factor in the case of the hydrodynamic force. Therefore, the dynamics of particle behavior depends on an interplay of collision-induced particle aggregation and cohesive force and the rate of aggregate breakage due to the hydrodynamic stress.

The aggregate cohesive strength τ is a function of the physicochemical and biological conditions as well as the aggregate properties, while the hydrodynamic stress σ depends on the design of the aggregation unit and the prevailing process conditions. Several empirical and theoretical formulations are available for predicting the aggregate cohesive force and the maximum hydrodynamic breaking force. The global hydrodynamic stress σ due to the shearing action of the fluid motion on the aggregate as well as the overall cohesive strength τ of the aggregate resisting the hydrodynamic loading assuming a uniform shape and constant porosity can be expressed mathematically in Eqs. (10) and (11) [25, 26]. An equilibrium of particle dynamics is reached at the steady-state condition. In this state, a continued particle or micro flocs/aggregate attachment to the larger flocs/aggregate is prevented, or the breakup kinetics is equal to the turbulence-induced collision rates.

In assessing aggregate strength and resistance to hydrodynamic-induced breakup, two common approaches are normally followed namely: limiting growth and limiting strength. The former relies on the determination of the maximum floc size before rupture, while the latter is based on the micromechanical analysis of aggregate strength. Many empirical and theoretical formulations based on the mentioned approaches are available in literature (Eqs. (12) and (13)). Liu et al. [27] presented the yield stress approach for calculating maximum aggregate tensile strength τ_y at which breakage is likely to occur in the inertia range of turbulence (Eq. (12)). Similarly, Attia [28] presented a model for predicting the critical fluid velocity above which there will be aggregate disruption by estimating floc yield stress σ_y resulting from the dynamic pressure acting on the floc (Eq. (13)).

$$\sigma = \mu G = \mu \sqrt{\frac{\varepsilon}{\nu}} \quad (10)$$

$$\tau = \frac{(1-p)F_B}{pd_p^2} \quad (11)$$

$$\tau_y = \frac{F_B}{d_p^2} \left(\frac{\lambda_0}{d_F} \right)^k \quad (12)$$

$$\sigma_y = \frac{1}{2} \rho_f v^2 \quad (13)$$

5. Case studies in environmental and biological systems

This section presents a short review of the recent studies on the applications of turbulence or hydrodynamics in the environmental and biological systems (**Table 2**). Water purification, irrigation, water quality assessment, sludge dewatering, bio-flocculation, and bio-clogging are some of the technical areas of application identified.

Technical application	Flow regime	Study type	References
Biofouling/biofilms	Turbulent	Experimental/CFD	[25–30]
Water disinfection/irrigation	Turbulent	Experimental/CFD	[31–35]
Water self-purification	Turbulent	Experimental	[43–46]
Solid-liquid separation	Turbulent	Experimental	[2, 36–38]
Food and paper processing	Turbulent	Experimental	[39–42]

Table 2.

Selected studies on computational and experimental studies of turbulence applications in environmental and biological processes.

It should be noted that improvements in the performance of the engineered processes (e.g., stirred tanks, shear reactors and photobioreactors etc.) in the identified areas of applications continue to shape the research focus in the field of environmental process engineering [29]. In this respect, studies have been conducted to determine how to accurately quantify the impact of hydrodynamic characteristics on the infectivity of bacteriophage MS2, a norovirus surrogate. Several studies also involved the development of bioreactors for testing the effect of hydrodynamic characteristics on microalgae and human enteric viruses [29–33]. The results obtained from the studies indicated that the hydrodynamic cavitation could trigger the inactivation waterborne viruses to levels defined in water quality directives. This was reportedly due to OH-radicals that form an AOP during the cavitation process and high shear forces inside the cavitation structure. Also, flow structures in a hydrodynamic filter have been numerically investigated [34]. In this study, tangential component of velocity was defined, and the three-dimensional pattern of the flow current/streamlines was obtained using their two-dimensional projection in the meridian cross-section of the filter, which allows one to discover the vortex structures. It was concluded that the optimal flow regime can be implemented by selecting the optimal correlation between the flow of liquid regime to be processed and the rotation frequency of the filtering baffle in the hydrodynamic filter. The remaining sub-sections describe how hydrodynamics, turbulence, and vortex dynamics are applied to achieve the desired process efficiency in other identified areas of applications—water purification, sludge dewatering, food processing, and self-purification of the water bodies.

5.1 Hydrodynamics in water purification process

In fluid engineering problems, research has consistently focused on identifying parameters that improve engineered processes including water purification and inactivation of pathogens [35]. While the conventional technique of disinfection by chlorination has been employed to kill pathogenic microorganisms in raw water, recent studies have shown that chlorine reacts with organic compounds in water and generates disinfection byproducts (DBPs), such as trihalomethanes (THMs), haloacetic acids (HAAs), etc. As a result, turbulence-induced inactivation has been studied as an alternative approach.

The effect of hydrodynamic parameters such as orifice size, orifice number and orifice layout of multi-orifice plate, cavitation number, cavitation time and orifice velocity on the microbial population have been investigated to determine how the desired process efficiency can be achieved [36]. Experimental results have shown that cavitation effects increased with decrease in orifice size and increase in orifice number, cavitation time and orifice velocity. Flow hydrodynamics and pipe material have also been shown to influence biofilm development in drinking water distribution systems (DWDS). Furthermore, biofilm development was inhibited at higher

flows indicating shear forces imposed by the flow conditions were above the critical levels for biofilm attachment. Experimental data from these studies were used to characterize the hydrodynamic behavior for numerical simulation and validation [37, 38]. Low-cost pipe-based pathogen reduction system was also demonstrated by Thomas et al. Their approach has a huge potential for application in developing countries due to its simple design [39].

5.2 Hydrodynamics in solid-liquid separation

In the design of process reactors, it is often necessary to tailor the separation technique to the dynamics and characteristics of the waste slurry that is being treated. Hence, several studies have been conducted to determine the influence of hydrodynamics on sludge processing. The optimum dosage values, which were obtained when flocculation performance was assessed based on surrogate indicators such as sludge volume index and supernatant turbidity, confirmed polymer bridging as the primary flocculation mechanism. Specific apparatus construction and reactor geometry were found to help maintain sludge suspension in a metastable state that is crucial for the formation of pellet-like compact agglomerates with better dewaterability properties [2, 40]. Similarly, sludge disintegration, using rotor-stator type hydrodynamic cavitation reactor (HCR), has been experimentally investigated [41]. To determine the effects of cavitation (including thermal energy) and shear stress on sludge disintegration, the performance of the HCR with and without the dimples and temperature control was analyzed. The results indicated that when dimples were present and there was no temperature control, the reduction of sludge particles increased by 50–80%. Further, the disintegration performance increased with the rotational speed and was minimized at the highest inlet pressure. Several other studies leveraging on the hydrodynamics of the process reactor for fluid-particle separation are available in literature [42, 43]. Many of these lab-scale studies have demonstrated the feasibility of turbulence-induced fluid-particle separation.

5.3 Hydrodynamics in food and paper processing

Hydrodynamic cavitation (HC) is a process in which high energy is released in a flowing liquid upon bubble implosion due to decrease and subsequent increase in local pressure. In food and beverage industries, hydrodynamic cavitators can be utilized for the purpose of extraction, emulsification, sterilization, disinfection, and homogenization [44]. HC, which can effectively induce sonochemistry by mechanical means, creates extraordinarily high of pressures of ~1000 bar, local hotspots with ~5000 K, and high oxidation (hydroxyl radicals) in room environment, without introducing new chemicals. For possible industrial application, the efficiency of HC has been studied by comparing the chemical oxygen demand (COD) removal efficiency of a Venturi device to that of an orifice plate. A sucrose solution and an effluent from a sucrose-based soft drink industry were treated. Results showed that the Venturi device recorded 90% COD removal efficiency after treatment period of three minutes. On the other hand, the orifice plate recorded 90% COD removal efficiency after 9 minutes [44–46]. Developing high-performance HCRs and revealing the corresponding disinfection mechanisms constitute the most crucial issues today [45].

Refining of cellulose pulp is a critical step in obtaining high quality paper characteristics, however, this process is slow and costly especially for refining longer conifer fibers which are the preferred source for high quality paper production and give the paper its strength. Recently, hydrodynamic cavitation was applied to the refinement conifer rich pulp samples [47].

5.4 Hydrodynamics in self-purification of water bodies

The self-purification ability of water bodies is related to the prevailing hydrodynamic conditions. Coupled hydrodynamic and water quality models have been used to investigate the spatial and temporal water quality variations of the water bodies. Using an Acoustic Doppler Velocimeter, the efficiency of aeration plug-flow device (APFD) in terms of water flow and dissolved oxygen (DO) have been determined experimentally [48–50]. Recent findings have shown that discharges from several rivers flowing into the New York/New Jersey (NY/NJ) harbor interact and interfere with one another. Such interactions can improve or inhibit water and contaminant flushing from the harbor. In Poyang Lake, three-dimensional velocity at various locations as well as the velocity distribution and turbulence characteristics were assessed, and plug-flow characteristics were analyzed. The two patterns of velocity and turbulence in horizontal sections observed are (1) near the aeration plug-flow device (APFD), the water flow was intensively pushed downstream and simultaneously recirculated; (2) farther away, the reflux area gradually decreased, and the velocity and turbulence distribution were more or less uniform. At the interfaces between two immiscible fluids – water and alkane of small carbon number, the amphiphilic PEO chain diffuses laterally, experiencing hydrodynamic drags from both phases. The absolute values of interfacial diffusion coefficients demonstrate a bigger contribution from the hydrodynamics from the water phase, which may be attributed to a stronger attraction between water and the PEO molecules [51].

5.5 Vortex patterns in fluid-particle reactors

The flow vortex patterns in many fluid-particle reactors are quite diverse and their analysis and characterization can provide an insight into the fluid and particle dynamics within the reactor. One important feature in many of these flow types is the presence of rotation or swirling or a combination of both resulting in anisotropic turbulence. A few of the dominant vortex patterns will be discussed in this section. It is also worth mentioning that the flow pattern is a function of the reactor geometry, stirrer or agitator, baffles, and the operating conditions. The focus will be on the common reactor geometries and flow regimes that are typically encountered in many practical applications.

A qualitative and quantitative analysis of the flow pattern in a processing reactor may be performed experimentally using an optical diagnostic imaging technique such as PIV or PDA or by numerical modeling. The selected approach in a given scenario will depend on the required detail of the flow field as well as the available resources. While the latter provide a flexible option for the investigation of fluid flow problems, the former often complements or used in the validation of numerical model. A detailed description of specific techniques is beyond the scope of this submission. A few of the vortex patterns in some of these reactors are discussed below.

5.5.1 Rotatory flow vortex pattern (e.g., tubular reactor)

This type of flow pattern is commonly found in rotating tubular reactors with an enclosed flow induced by a stirrer. Previous studies have shown that this flow pattern has a profound influence on the performance of fluid-particle reactors, and this type of flow pattern can be found in many technical applications [29, 39, 52]. For instance, in terms of the stirrer-vessel configuration, the flocculation performance is significantly influenced by the impeller type and its speed. The axial impeller has been found to promote floc formation over a range of impeller speeds as it produces

a more homogeneous distribution of local velocity gradients in comparison to the radial impeller. Also, high velocity gradients occur in the region around the impeller, which might significantly hamper the high rate activated sludge (HRAS) flocculation process [53, 54].

5.5.2 Oscillatory flow vortex pattern (e.g., oscillatory reactor)

An oscillator is a device whose action causes intermittent velocity gradients over time, space, and direction, and can be used for colloid removal based on physical flow manipulation. An oscillatory flow pattern is commonly found in reactors with an enclosed flow induced by an oscillator. Results from previous studies have shown that gentle oscillation can promote simultaneous flocculation and particle agglomeration over a relatively short periods of time [42]. This technique, whose implementation can result in reductions of the reactor sizes and process times, has a strong potential to improve conventional separation processes. It has also been observed that higher oscillating frequency promotes faster upward vertical velocities, resulting in different sedimentation patterns and removal efficiencies generated by the different oscillation frequencies [43].

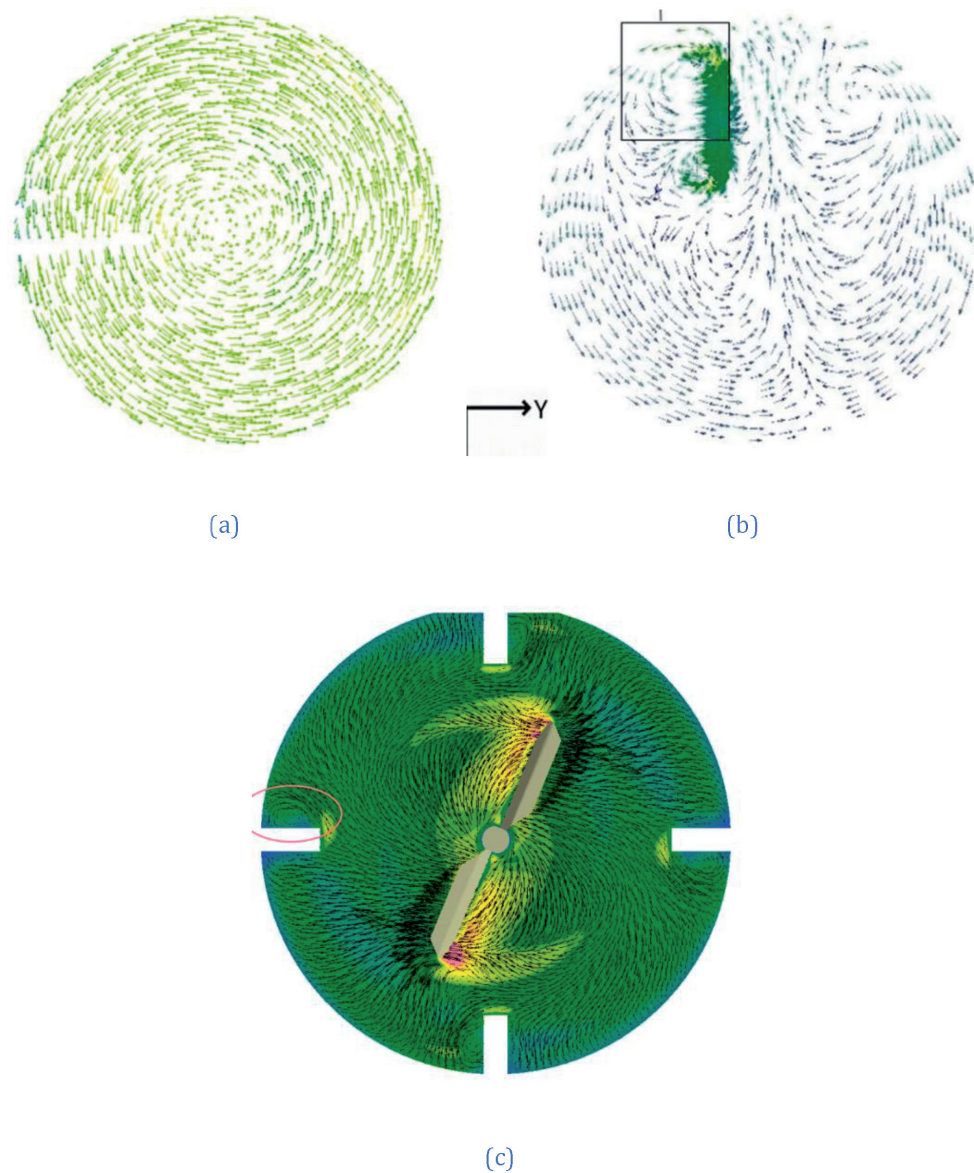


Figure 6. Typical cross-sections of vortex patterns in fluid-particle reactors (a) rotatory-type flow field (b) oscillatory-type flow field (c) swirling-type flow field.

5.5.3 Swirling flow vortex pattern (e.g., stirred tank, hydrocyclone)

A swirling type of flow pattern is commonly found in hydrocyclone [55–57] and counter-rotating reactors with an enclosed flow induced by a rotational swirling effect [58, 59]. In addition to hydrocyclone, this type of flow field is also common in rotating reactors with baffles such as mixing tank, in which case, the flow is a combination of rotational and swirl dominated flow as shown in **Figure 6c**. In the case of a counter-rotating vortex reactor, it has also been found that the swirl ratio and micromixing time of the flow increases as the vortex reactor (MIVR) is scaled up, indicating a flow with stronger swirl yet less mixing efficiency [60]. In order to promote mixing and enhance the floc formation process, some baffles should be installed to break water flow co-rotation with the impeller [54]. In modifying the flow pattern to suit a particular condition, it is advisable to perform the optimization of the impeller shape for a particular vessel geometry [61, 62].

6. Conclusions and future perspectives

This brief communication is a summary of the main concepts involved the fluid-particle research and technical applications. It is by no means an exhaustive contribution and readers interested in the details of the subject-matter are advised to consult other scientific information available on the subject-matter. The fluid process engineering is a field of active research and there is an ever-increasing scope for the application of hydrodynamics, turbulence, and vortex dynamics. In addition to the identified areas of application, there are several emerging areas of application. As the turbulence research advances with better computing power and algorithms, it is hoped that there will be limitless scope for the application of vortex dynamics in fluid process engineering.

Conflict of interest

The authors declare no conflict of interest.

Nomenclature

APFD	aeration plug-flow device
COD	chemical oxygen demand
DBPs	disinfection byproducts
DO	dissolved oxygen
DWDS	drinking water distribution systems
HAAs	haloacetic acids
HC	hydrodynamic cavitation
HCR	hydrodynamic cavitation reactor
THMs	trihalomethanes

IntechOpen

Author details


Benjamin Oyegbile^{1*}, Brian Oyegbile² and Guven Akdogan¹

1 Department of Process Engineering, Faculty of Engineering, Stellenbosch University, Stellenbosch, South Africa

2 College of Engineering, University of Georgia, Athens, GA, USA

*Address all correspondence to: hollander196@yahoo.com

IntechOpen

© 2020 The Author(s). Licensee IntechOpen. This chapter is distributed under the terms of the Creative Commons Attribution License (<http://creativecommons.org/licenses/by/3.0>), which permits unrestricted use, distribution, and reproduction in any medium, provided the original work is properly cited. 

References

- [1] Crowe CT, Truitt TR, Chung JN. In: Green SI, editor. *Fluid Vortices*. Dordrecht: Springer; 1995. pp. 829-861. DOI: 10.1007/978-94-011-0249-0_19
- [2] Oyegbile BA. *Optimization of Micro Processes in Fine Particle Agglomeration by Pelleting Flocculation*. Leiden: CRC Press; 2016. DOI: 10.1201/9781315671871
- [3] Oyegbile B, Ay P, Narra S. Flocculation kinetics and hydrodynamic interactions in natural and engineered flow systems: A review. *Environmental Engineering Research*. 2016;21:1-14. DOI: 10.4491/eer.2015.086
- [4] Oyegbile B, Akdogan G, Karimi M. Modelling the dynamics of granular particle interactions in a vortex reactor using a coupled DPM-KTGF model. *South African Journal of Chemical Engineering*. 2020;34:31-46. DOI: 10.1016/j.sajce.2020.05.008
- [5] Morchain J. *Bioreactor Modeling*. Oxford: Elsevier; 2017. pp. 29-84. DOI: 10.1016/b978-1-78548-116-1.50002-1
- [6] Paul EL, Atiemo-Obeng VA, Kresta SM, editors. *Handbook of Industrial Mixing: Science and Practice*. Hoboken, NJ: John Wiley & Sons; 2004. DOI: 10.1002/0471451452
- [7] Harun Z, Lotfy ER. In: Barille R, editor. *Turbulence and Related Phenomena*. London: InTech Open; 2019. DOI: 10.5772/intechopen.76854
- [8] Yeoh GH, Cheung CP, Tu J. *Multiphase Flow Analysis Using Population Balance Modeling: Bubbles, Drops and Particles*. Waltham, MA: Butterworth-Heinemann; 2014
- [9] Peker SM, Helvacı ŞŞ, Yener HB, İvizler B, Alparslan A, editors. *Solid-Liquid Two Phase Flow*. Oxford: Elsevier; 2008. DOI: 10.1016/b978-0-444-52237-5.x5001-2
- [10] Hendricks D. *Fundamentals of Water Treatment Unit Processes*. Boca Raton, FL: CRC Press; 2011. DOI: 10.1201/9781439895092
- [11] Zlokarnik M. *Stirring: Theory and Practice*. Weinheim: Wiley-VCH; 2008
- [12] Kockmann N. *Transport Phenomena in Micro Process Engineering*. Heidelberg: Springer; 2008
- [13] Oldshue JY, Trussell RR, Trussell R. Design of Impellers for mixing. In: Amirtharajah A, Clark MM, Trussell R, editors. *Mixing in Coagulation and Flocculation*. Denver, CO: American Water Works Association; 1991. pp. 309-342
- [14] Logan BE. *Environmental Transport Processes*. Hoboken, NJ: John Wiley & Sons; 2012
- [15] Bache DH, Gregory R. *Flocs in Water Treatment*. London: IWA Publishing; 2007. DOI: 10.2166/9781780402000
- [16] Bratby J. *Coagulation and Flocculation in Water and Wastewater Treatment*. London: IWA Publishing; 2016
- [17] Yeoh GH, Tu J. *Computational Techniques for Multiphase Flows*. 2nd ed. Oxford: Elsevier; 2019
- [18] Taboada-Serrano P, Chin C-J, Yiaccoumi S, Tsouris C. Modeling aggregation of colloidal particles. *Current Opinion in Colloid & Interface Science*. 2005;10:123-132. DOI: 10.1016/j.cocis.2005.07.003
- [19] Gregory J. *Particles in Water: Properties and Processes*. Boca Raton, FL: CRC Press; 2006. DOI: 10.1201/9780203508459
- [20] Norouzi HR, Zarghami R, Sotudeh-Gharebagh R, Mostoufi N.

Coupled CFD-DEM Modeling: Formulation, Implementation and Application to Multiphase Flows. Chichester: John Wiley & Sons; 2016. DOI: 10.1002/9781119005315

[21] Crowe CT, Schwarzkopf JD, Sommerfeld M, Tsuji Y. Multiphase Flows with Droplets and Particles. Boca Raton, FL: CRC Press; 2011. DOI: 10.1201/b11103

[22] Thomas DN, Judd SJ, Fawcett N. Flocculation modelling: A review. *Water Research*. 1999;**33**:1579-1592. DOI: 10.1016/s0043-1354(98)00392-3

[23] Marshall JS. Effect of particle collisions on the expulsion of heavy particles from a vortex core. *Physics of Fluids*. 2006;**18**:113301. DOI: 10.1063/1.2370427

[24] Sun R, Xiao H, Sun H. Investigating the settling dynamics of cohesive silt particles with particle-resolving simulations. *Advances in Water Resources*. 2018;**111**:406-422. DOI: 10.1016/j.advwatres.2017.11.012

[25] Coufort C, Bouyer D, Liné A. Flocculation related to local hydrodynamics in a Taylor–Couette reactor and in a jar. *Chemical Engineering Science*. 2005;**60**:2179-2192. DOI: 10.1016/j.ces.2004.10.038

[26] Shamlou PA, Titchener-Hooker N. *Processing of Solid–Liquid Suspensions*. Oxford: Butterworth-Heinemann; 1993. pp. 1-25. DOI: 10.1016/b978-0-7506-1134-3.50005-3

[27] Liu SX, Glasgow LA. Aggregate disintegration in turbulent jets. *Water, Air, and Soil Pollution*. 1997;**95**:257-275. DOI: 10.1007/bf02406169

[28] Attia YA, Laskowski JS, Ralston J. Flocculation. In: *Colloid Chemistry in Mineral Processing*. Amsterdam: Elsevier; 1992. pp. 277-308

[29] Zhang Q, Wu X, Xue S, Liang K, Cong W. Study of hydrodynamic characteristics in tubular photo-bioreactors. *Bioprocess and Biosystems Engineering*. 2012;**36**:143-150. DOI: 10.1007/s00449-012-0769-2

[30] Kosel J, Gutiérrez-Aguirre I, Rački N, Dreo T, Ravnikar M, Dular M. Efficient inactivation of MS-2 virus in water by hydrodynamic cavitation. *Water Research*. 2017;**124**:465-471. DOI: 10.1016/j.watres.2017.07.077

[31] Zhang QH, Wu X, Xue SZ, Wang ZH, Yan CH, Cong W. Hydrodynamic characteristics and microalgae cultivation in a novel flat-plate photobioreactor. *Biotechnology Progress*. 2012;**29**:127-134. DOI: 10.1002/btpr.1641

[32] Yan H, Guan C, Jia Y, Huang X, Yang W. Mixing characteristics, cell trajectories, pressure loss and shear stress of tubular photobioreactor with inserted self-rotating helical rotors: Mixing characteristics, cell trajectories, pressure loss and shear stress. *Journal of Chemical Technology and Biotechnology*. 2017;**93**:1261-1269. DOI: 10.1002/jctb.5484

[33] Muller-Feuga A, Pruvost J, Guédes RL, Déan LL, Legentilhomme P, Legrand J. Swirling flow implementation in a photobioreactor for batch and continuous cultures of *porphyridium cruentum*. *Biotechnology and Bioengineering*. 2003;**84**:544-551. DOI: 10.1002/bit.10818

[34] Devisilov VA, Sharai EY. Numerical study of the flow structure in a hydrodynamic filter. *Theoretical Foundations of Chemical Engineering*. 2016;**50**:209-216. DOI: 10.1134/s0040579516020044

[35] Baranova MP. Hydrodynamic cavitation unit for improving the performance of irrigation water

during plant growing. IOP Conference Series: Earth and Environmental Science. 2019;**315**:062018. DOI: 10.1088/1755-1315/315/6/062018

[36] Kudryashova T, Polyakov S, Tarasov N. A novel parallel algorithm for 3D modelling electromagnetic purification of water. MATEC Web of Conferences. 2018;**210**:04027. DOI: 10.1051/mateconf/201821004027

[37] Dong Z, Zhao W. Killing rate of colony count by hydrodynamic cavitation due to square multi-orifice plates. IOP Conference Series: Earth and Environmental Science. 2018;**121**:022004. DOI: 10.1088/1755-1315/121/2/022004

[38] Cowle MW, Webster G, Babatunde AO, Bockelmann-Evans BN, Weightman AJ. Impact of flow hydrodynamics and pipe material properties on biofilm development within drinking water systems. Environmental Technology. 2019;**1**:1-13. DOI: 10.1080/09593330.2019.1619844

[39] Thomas SF, Rooks P, Rudin F, Cagney N, Balabani S, Atkinson S, et al. Swirl flow bioreactor containing dendritic copper-containing alginate beads: A potential rapid method for the eradication of *Escherichia coli* from waste water streams. Journal of Water Process Engineering. 2015;**5**:6-14. DOI: 10.1016/j.jwpe.2014.10.010

[40] Oyegbile B, Ay P, Narra S. Optimization of physicochemical process for pre-treatment of fine suspension by flocculation prior to dewatering. Desalination and Water Treatment. 2016;**57**:2726-2736. DOI: 10.1080/19443994.2015.1043591

[41] Kim H, Koo B, Sun X, Yoon JY. Investigation of sludge disintegration using rotor-stator type hydrodynamic cavitation reactor. Separation and Purification Technology. 2020;**240**:116636. DOI: 10.1016/j.seppur.2020.116636

[42] Halfi E, Brenner A, Katoshevski D. Separation of colloidal minerals from water by oscillating flows and grouping. Separation and Purification Technology. 2019;**210**:981-987. DOI: 10.1016/j.seppur.2018.08.054

[43] Halfi E, Arad A, Brenner A, Katoshevski D. Development of an oscillation-based technology for the removal of colloidal particles from water: CFD modeling and experiments. Engineering Applications of Computational Fluid. 2020;**14**:622-641. DOI: 10.1080/19942060.2020.1748114

[44] Asaithambi N, Singha P, Dwivedi M, Singh SK. Hydrodynamic cavitation and its application in food and beverage industry: A review. Journal of Food Process Engineering. 2019;**42**. DOI: 10.1111/jfpe.13144

[45] Sun X, Liu J, Ji L, Wang G, Zhao S, Yoon JY, et al. A review on hydrodynamic cavitation disinfection: The current state of knowledge. Science of the Total Environment. 2020;**737**:139606. DOI: 10.1016/j.scitotenv.2020.139606

[46] Alves PHL, de Silva PSL, Ferreira DC, de Gonçalves JCSI. COD removal from sucrose solution using hydrodynamic cavitation and hydrogen peroxide: A comparison between Venturi device and orifice plate. RBRH. 2019;**24**. DOI: 10.1590/2318-0331.241920180147

[47] Kosel J, Šinkovec A, Dular M. A novel rotation generator of hydrodynamic cavitation for the fibrillation of long conifer fibers in paper production. Ultrasonics Sonochemistry. 2019;**59**:104721. DOI: 10.1016/j.ultsonch.2019.104721

[48] Li B, Yang G, Wan R, Li H. Hydrodynamic and water quality

- modeling of a large floodplain Lake (Poyang lake) in China. *Environmental Science and Pollution Research*. 2018;**25**:35084-35098. DOI: 10.1007/s11356-018-3387-y
- [49] Li Y, Feng H, Zhang H, Sun J, Yuan D, Guo L, et al. Hydrodynamics and water circulation in the New York/New Jersey Harbor: A study from the perspective of water age. *Journal of Marine Systems*. 2019;**199**:103219. DOI: 10.1016/j.jmarsys.2019.103219
- [50] Li X, Huang M, Wang R. Numerical simulation of Donghu Lake hydrodynamics and water quality based on remote sensing and MIKE 21. *ISPRS International Journal of Geo-Information*. 2020;**9**:94. DOI: 10.3390/ijgi9020094
- [51] Li Z, Yang J, Hollingsworth JV, Zhao J. Lateral diffusion of single polymer molecules at interfaces between water and oil. *RSC Advances*. 2020;**10**:16565-16569. DOI: 10.1039/d0ra02630a
- [52] Visscher F, van der, Schaaf J, Nijhuis TA, Schouten JC. Rotating reactors – A review. *Chemical Engineering Research and Design*. 2013;**91**:1923-1940. DOI: 10.1016/j.cherd.2013.07.021
- [53] Bridgeman J, Jefferson B, Parsons SA. Computational fluid dynamics modelling of flocculation in water treatment: A review. *Engineering Applications of Computational Fluid*. 2014;**3**:220-241. DOI: 10.1080/19942060.2009.11015267
- [54] Balemans S, Vlaeminck SE, Torfs E, Hartog L, Zaharova L, Rehman U, et al. The impact of local hydrodynamics on high-rate activated sludge flocculation in laboratory and full-scale reactors. *PRO*. 2020;**8**:131. DOI: 10.3390/pr8020131
- [55] Mousavian SM, Najafi AF. Influence of geometry on separation efficiency in a hydrocyclone. *Archive of Applied Mechanics*. 2008;**79**:1033-1050. DOI: 10.1007/s00419-008-0268-8
- [56] Dai GQ, Li JM, Chen WM. Numerical prediction of the liquid flow within a hydrocyclone. *Chemical Engineering Journal*. 1999;**74**:217-223. DOI: 10.1016/s1385-8947(99)00044-3
- [57] Liu Y, Cheng Q, Zhang B, Tian F. Three-phase hydrocyclone separator – A review. *Chemical Engineering Research and Design*. 2015;**100**:554-560. DOI: 10.1016/j.cherd.2015.04.026
- [58] Derksen J. Confined and agitated swirling flows with applications in chemical engineering. *Flow, Turbulence and Combustion*. 2002;**69**:3-33. DOI: 10.1023/a:1022419316418
- [59] Jakirlic S, Hanjalic K, Tropea C. Modeling rotating and swirling turbulent flows: A perpetual challenge. *AIAA Journal*. 2002;**40**:1984-1996. DOI: 10.2514/2.1560
- [60] Liu Z, Ramezani M, Fox RO, Hill JC, Olsen MG. Flow characteristics in a scaled-up multi-inlet vortex nanoprecipitation reactor. *Industrial and Engineering Chemistry Research*. 2015;**54**:4512-4525. DOI: 10.1021/ie5041836
- [61] Jaszczur M, Młynarczykowska A, Demurtas L. Effect of impeller design on power characteristics and Newtonian fluids mixing efficiency in a mechanically agitated vessel at low Reynolds numbers. *Energies*. 2020;**13**:640. DOI: 10.3390/en13030640
- [62] Escamilla-Ruiz IA, Sierra-Espinosa FZ, García JC, Valera-Medina A, Carrillo F. Experimental data and numerical predictions of a single-phase flow in a batch square stirred tank reactor with a rotating cylinder agitator. *Heat and Mass Transfer*. 2017;**53**:2933-2949. DOI: 10.1007/s00231-017-2030-7